Characterizing nanoparticle release patterns of laser powder bed fusion in metal additive manufacturing: first step towards mitigation measures

Annals of Work Exposures and Health, 2022, **XX**, 1–14
https://doi.org/10.1093/annweh/wxac080
Advance access publication 23 November 2022
Original Article

Characterizing Nanoparticle Release Patterns of Laser Powder Bed Fusion in Metal Additive Manufacturing: First Step Towards Mitigation Measures

Roberta Pernetti[1,*], Francesco Galbusera[2], Alberto Cattenone[3], Enrico Bergamaschi[4], Barbara Previtali[2] and Enrico Oddone[1,5]

[1]Department of Public Health, Experimental and Forensic Medicine – University of Pavia, via Forlanini 2, 27100, Pavia, Italy;
[2]Department of Mechanical Engineering – Politecnico di Milano, Via La Masa 1, 20156, Milano, Italy;
[3]Department of Electrical, Computer and Biomedical Engineering – University of Pavia, via Ferrata 5, 27100, Pavia, Italy;
[4]Department of Public Health and Pediatrics, University of Turin, Piazza Polonia, 94, 10126, Turin, Italy;
[5]Hospital Occupational Unit of Occupational Medicine (UOOML) – ICS Maugeri IRCCS, Via Maugeri 10, 27100, Pavia, Italy

[*]Author to whom correspondence should be addressed. Tel: +39 0382 593802; e-mail: roberta.pernetti@unipv.it

Abstract

Laser Powder Bed Fusion (L-PBF) is a well-known Additive Manufacturing (AM) technology with a wide range of industrial applications. Potential occupational exposures to metal nanoparticles (NP) as by-products could occur in these processes, and no cogent occupational exposure limits are available. To contribute to this assessment, a monitoring campaign to measure the NP release pattern in two metal L-PBF facilities was carried out in two academic laboratories adopting L-PBF technology for research purposes. The monitored processes deal with two devices and three feedstock types, namely stainless steel (AISI 316L), aluminium-silicon alloy (A357) and pure copper, which are associated with different levels of industrial maturity. Prolonged environmental and personal real-time monitoring of NP concentration and size were performed, temperature and relative humidity were also measured during environmental monitoring. The measurements reveal a controlled NP release of the monitored processes, resulting in an average reduced exposure of the operators during the whole working shift, in compliance with proposed limit values (20 000 n cm^{-3} for density >6000 kg m^{-3} or 40 000 n cm^{-3} for density <6000 kg m^{-3}). Nonetheless, the monitoring results show release events with an increase in NP concentration and a decrease in NP size corresponding with several actions usually performed during warm-up and cleaning, leading to exposures over 40–50 000 n cm^{-3} during a considerable time interval, especially during the manufacturing of pure copper powder. The results show that the actions of the operators, boundary conditions (relative humidity) and set-up of the L-PBF device have an impact on the amount of NP released and their size. Several release events (significant increase in NP concentration and decrease in NP size) are identified and associated with specific job tasks of the workers as well as building conditions. These results contribute to the definition of NP release benchmarks in AM processes and provide information to improve the operational conditions of L-PBF processes as well as safety guidelines for operators.

Keywords: additive manufacturing; indoor air quality; metal nanoparticle exposure; occupational health

What's Important About This Paper?

Laser Power Bed Fusion is an emerging technology whose industrial application is increasing. This study conducted a real-time monitoring of the nanoparticles generated as by-product during six whole manufacturing processes adopting different metals and alloys as feedstock. The analysis identified the process actions and boundary conditions mainly affecting size and concentration of nanoparticles. The results move towards the definition of process benckmarks and appropriate mitigation measures to limit operators' exposures to nanoparticles during additive manufacturing processes.

Received: May 31, 2022. Accepted: October 24, 2022.

Introduction

Additive Manufacturing (AM) is an emerging technology that allows the production of complex objects through the addition of subsequent layers of material according to digital control based on 3D models (International Organization for Standardization, 2019). Metal AM processes are based on an energy source used to melt the metal powders according to the object design, enabling a reduction of the environmental impact of the production, and an increasing in process sustainability (Böckin and Tillman, 2019; Niaki *et al.*, 2019). According to the ISO/ASTM 52900:2021 (International Organization for Standardization, 2021), one of the main categories is Powder Bed Fusion (PBF), where the feedstock is a metallic round powder, evenly distributed onto a substrate plate using a coating mechanism, and selectively melted by a high energy source. When a laser beam is applied as the energy source, the process is called Laser Powder Bed Fusion (L-PBF).

The high energy for melting the powder, whose initial diameter usually ranges from 15 to 63 μm according to the composition and application, entails the release of fine, and nanoparticles (NP) of metal as a by-product of L-PBF processes (Kolb *et al.*, 2017). Despite the laser melting occurring in a sealed chamber, and the AM device usually being placed in a dedicated environment with mechanical ventilation, metal NP have been detected in proximity to the AM device (Jensen *et al.*, 2020; Sousa *et al.*, 2021). Moreover, the operators interact with the device for several activities e.g. handling powders, charging the tank, cleaning the components, and emptying the overflow container after the build job. These activities may lead to a potential exposure to metal particles and NP that may increase the risk of lung inflammation (Vallabani *et al.*, 2022) and asthma for the AM operators (Duffin *et al.*, 2007).

Besides the concentration, the aerodynamic diameter of generated particles represents one of the main factors affecting the likelihood of exposure, since the size influences the percentage of deposition along the respiratory airway: the finest particles can reach the gas exchange zone (i.e. the bronchioles and alveoli), and at nanoscale are also able to cross the air/blood barrier with an efficiency inversely correlated to the particle size (Kreyling *et al.*, 2014; Bengalli *et al.*, 2017). In addition, the disposal of nanoparticles from the body is more difficult due to the distribution to tissues other than the lung and the large surface area of interaction with biological structures (Duffin *et al.*, 2007). The particle size also influences the exposure pattern, affecting the deposition time and the persistence in the working environment (Kuijpers *et al.*, 2017). NP are characterised by a slow sedimentation rate (Fonseca *et al.*, 2016; Mellin *et al.*, 2016) and can be detected for several hours after the end of the building process (Shi *et al.*, 2015), also depending on ventilation rate and relative humidity (Wang *et al.*, 2017).

Previous reviews (Sousa *et al.*, 2019; Chen *et al.*, 2020) highlight only few studies investigating NP exposure in AM facilities through real-time on-field monitoring, pointing out the need to further characterise the release of NP as by-products, from physical, chemical and toxicological perspectives (Wang *et al.*, 2021).

The current references developed by ACGIH (American Conference of Governmental Industrial Hygienists, 2021), OSHA (Occupational Safety and Health Administration, 2020) and NIOSH (National Institute of Occupational Safety and Health, 2007) for metal exposure are based on traditional technologies (such as welding, grinding, melting) and prescribe mass evaluation. Therefore, these limits do not provide an effective assessment of the release in terms of size and concentration and a proper hazard evaluation. A recent study reported a case in one AM facility where the metal concentrations complied with the limits assessed through gravimetric evaluation. Nevertheless, further analyses on AM operators' urine presented a concentration of chromium, cobalt and nickel 20–30% higher than the administrative personnel of the company (Ljunggren *et al.*, 2019), thus highlighting the exposure.

There is the need for systematic studies on different metal AM settings in order to characterise particle release and provide a structured knowledge about their features and distribution over time and space, in order to support the definition of benchmarks and standardised exposure limits (Van Broekhuize *et al.*, 2012). In this regard, the authors performed a preliminary measurement campaign based on standard gravimetric analysis to evaluate the respirable and inhalable dust in the monitored sites (Oddone *et al.*, 2022). The results of the gravimetric analysis showed concentrations 5–100 times lower than the threshold limit values (TLVs) for the analysed metals, while the results of the particle count (0.3–25 μm) were in line with (Ljunggren *et al.*, 2019) who also detected the release of nanoparticles. Therefore, the aim of this study is to complete the characterisation of AM emissions carried out by Oddone (see Oddone *et al.*, 2022) by focusing on nanoparticles, whose monitoring and quantification is reported only in few studies, in order to identify the pattern of release and the activities entailing an increase in the concentration as well as a reduction in the particle size.

The relevance of this work lies in the presentation of data from the prolonged monitoring of operative conditions of AM processes, including deviations from the standard procedures and malfunctioning.

The monitored processes apply three alloys associated with a different level of maturity in the AM application: (i) stainless steel (AISI 316L) that has been widely investigated and is commonly adopted in industrial AM settings with standard process parameters; (ii) aluminium-based alloy (A357) that presents several potential applications and which is at an advanced research phase for the definition of proven process parameters; (iii) pure copper (Cu), whose application in AM is still at the research phase for defining effective process parameters.

Materials and methods

Main features of AM sites

The two monitored devices in the Politecnico di Milano (POLIMI) and the University of Pavia (UNIPV) are used for research on process optimisation. Both systems are L-PBF architectures, entailing the addition of a series of powder layers ranging from a thickness of 20–60 μm, depending both on the processed material and the building plate that is melted by the laser beam according to the job design. The processes of the printer 3D-NT LLA150 (Prima Additive, Torino, Italy) were analysed in POLIMI, while the processes with the printer Renishaw AM250 (Renishaw, Stone, UK) were monitored in UNIPV. The first machine is an open L-PBF system, with the ability to operate the laser source in different modes (pulsed and continuous wave emission) and to process new and non-commercial powders while varying process parameters, scanning strategy and inert gas type. The second system is more rigid and consolidated, processing standard powders according to the manufacturer's specifications.

Prior to manufacturing, the build chamber is filled with argon, and the oxygen content is maintained at 2300 ppm for the POLIMI machine and below 1000 ppm for the UNIPV machine (i.e. inertisation). The excess powder is funnelled into the overflow container and removed during the cleaning operation to be sieved and reused in further processes.

The two sites have different boundary conditions. POLIMI presents an open-space laboratory with separated metal boxes (surface 5.4 m^2) for each AM device. The boxes are conditioned and ventilated by a central mechanical system that ensures a complete air change rate of the room every 4 min (approx. 0.25 vol min^{-1}). The device in UNIPV is installed in a dedicated room (surface 8.5 m^2) with a local climate-control system and natural ventilation.

Monitoring approach

The monitoring campaign focused on the measurement of real-time nanoparticle concentrations released during the whole building processes. The monitoring was performed through one Miniature Diffusion Size Classifier (DiSCMini—TESTO), based on the measurement of the induced unipolar charging of the particles flowing through two subsequent electrometer stages. It allowed the quantification of the particle concentration in the sampled air [n cm^{-3}, number of particles per air sample volume] and the average particle size [nm] within the range 10–300 nm (Fierz *et al.*, 2011). Both environmental monitoring (ENV), by positioning the sensors next to the build chamber door, and personal monitoring (PERS) sampling in the breathing zone of the operators were conducted.

The environmental monitoring dealt with the whole manufacturing process that, for the purposes of this work, is divided into four phases and summarised in Fig. 1:

- *Warm-up (open chamber)*: preliminary activities for launching the build job: preparation of the build chamber, calibration of the re-coater, charging of raw powders, device general settings;
- *Building (closed chamber)*: including inertisation and de-inertisation operations and the process entailing the use of the laser to build the object;
- *Pause (closed chamber)*: time intervals from the end of the build job to the beginning of cleaning or after cleaning;
- *Cleaning (open chamber)*: removal of the substrate, removal of the built object, cleaning of the build volume with brushes and vacuum to remove small quantities of powder deposited in the mechanic gaps, emptying of the overflow container and cleaning of the filters.

As shown in Fig. 1, the operators during warm-up and cleaning use to wear personal protection equipment, namely nitrile disposable gloves, full-body protective suit, and full-face respirator mask with aerosol and particle filter class 3 according to EN 143:2021(Comité Européen de Normalisation, 2021).

The personal monitoring dealt with the phases with a direct interaction between the operators and the manufacturing system, namely warm-up, and cleaning. Coupled with the environmental monitoring of NP, a datalogger 174-H (Testo) was adopted for measuring the air temperature (accuracy ± 0.5°C) and relative humidity (accuracy ± 3%) in the 3D system dedicated box.

The environmental background of airborne NP was estimated by measuring the concentration of NP in proximity for a time interval of 5′ and on the desks used by the operators during the building process. More details concerning the chemical composition and properties of the powder feedstock's are summarised in supplementary materials.

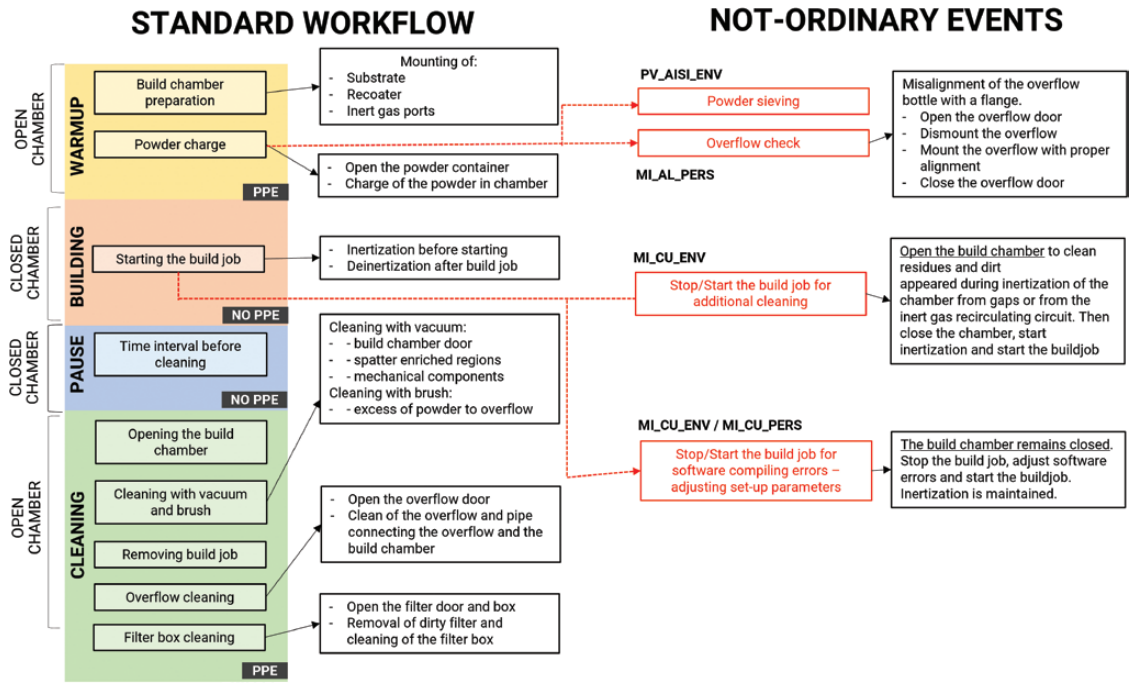

Figure 1. Flowchart of a standard L-PBF process and job tasks with the identification of non-ordinary events during the monitoring campaign. PPE/NO PPE indicate respectively that the operators wear and do not wear personal protection equipment.

Statistical analysis

The normal distribution of variables (nanoparticle number and size, air temperature, and relative humidity) was checked by the Shapiro–Wilk test. Since these continuous variables are not normally distributed, they were described in terms of median and interquartile range. Statistical differences between median values of considered variables were tested by the Kruskall–Wallis method. Correlations between the number and size of NP, air temperature, and relative humidity were carried out using regression coefficients (β) calculated according to the quantile regression method. The significance level was set at alpha 0.01 (statistical significance at $P < 0.01$), and two-tailed tests were always used. The analyses were conducted with STATA software (version 14; Stata Corporation, College Station, TX, USA, 2015).

Results

The data were collected through different monitoring sessions from July 2021 to January 2022, with a focus on sample days representing the usual operation in an AM facility. Supplementary Table SM1 in supplementary materials reports the nominal chemical compositions, density and granulometry of the powders processed during the experimental activity. In each building phase, the samples were built upon proper substrates, whose material was a stainless steel for AISI316L and pure Cu powders and aluminium for A357. Table 1 shows an overview of the six monitored processes in terms of monitoring types and phases with their corresponding lengths.

The box plot charts of the environmental monitoring (Fig. 2) highlight a general increase in the nanoparticle concentration with respect to the background (values in dotted line). The process presenting the higher release is MI_A357_ENV, with an average +36% of concentration with respect to the background, while MI_Cu_ENV showed +20% and PV_316L_ENV +9%, considering the average values of all the monitored phases. The highest increases with respect to the background were collected when pure Cu powder (+60%) and A357 (+104%) were adopted as feedstock, corresponding to an enhancing of the particle concentration respectively of + 3120 n cm^{-3} and 5540 n cm^{-3} (for more detailed data please refer to Tables SM2 and SM3 of Supplementary materials). This increase occurs during the building phase, when the build chamber is sealed and filled with argon and its recirculation system should filter the powders.

The results show a different pattern of release for each powder. MI_Cu_ENV presents large interquartile ranges representing frequent variations, mainly increases, with respect to the average concentration and a more constant release during the warm-up and

Table 1. Overview of the monitored processes in terms of monitoring type and phases, and warm-up, building and cleaning lengths

Process	Location	Date	Type	Phases	Duration of the monitored phases		
					Warm-up	Building	Cleaning
PV_316L_ENV	PV	07/21	Environmental	Whole process	55′	30 h	2h + 3h 40′
PV_316L_PER		12/21	Personal	Warm-up cleaning	1h 28′	–	40′
MI_A357_PERS	POLIMI	11/21	Personal	Warm-up cleaning	40′	–	2h 20′
MI_A357_ENV		11/21	Environmental	Whole process	50′	3h 52’	1h 08′
MI_Cu_ENV		12/21	Environmental	Whole process	2h 39′	5 h	1h 31′ + 1 h 34′
MI_Cu_PERS		01/22	Personal	Warm-up cleaning	2h 4′	–	2h 54′
MI_Cu_ENV_2		01/22	Environmental	Building	–	10 h	–

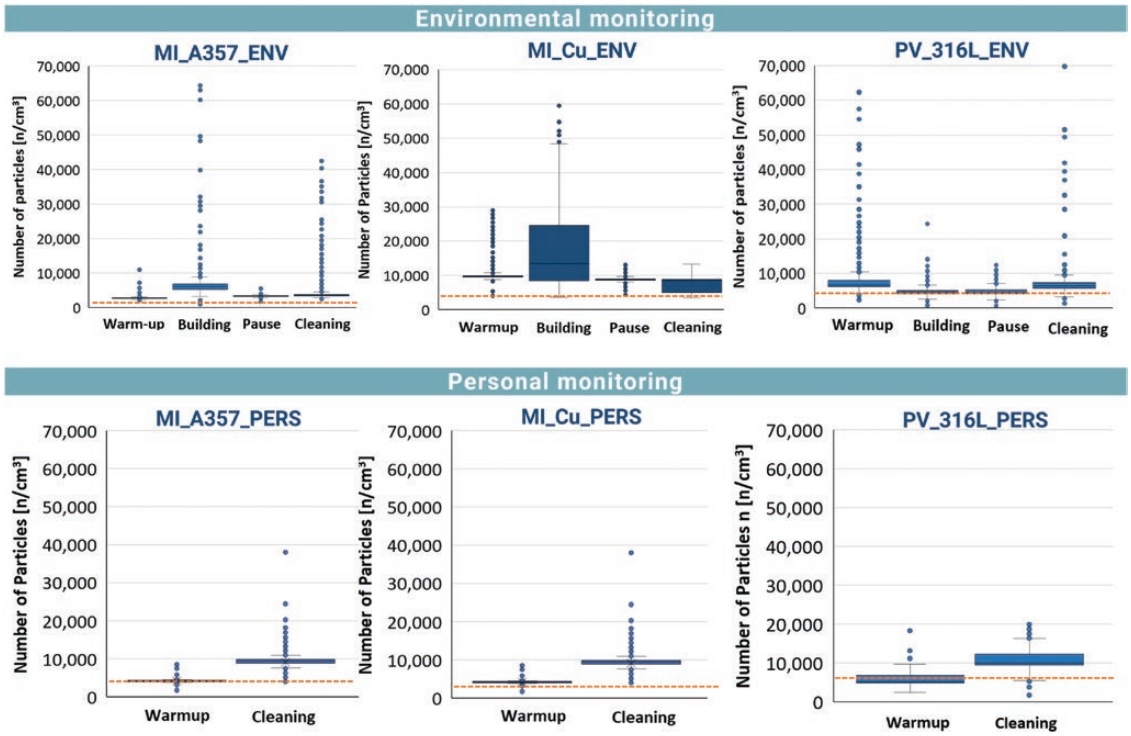

Figure 2. Environmental and personal monitoring of particle concentration expressed in n cm^{-3} as a function of the phase (dotted line shows the background concentration).

building. MI_A357_ENV and PV_316L_ENV show a comparable pattern of release with reduced interquartile ranges, lying within concentrations lower than 10 000 n cm^{-3} (which is not exceeded by the whiskers either). On the other hand, several values above the whiskers are observed meaning that, in general, MI_A357_ENV and PV_316L_ENV present in general a reduced release during the process phases that is coupled with significant peaks corresponding to release events.

Figure 2 also shows the boxplot for personal monitoring (warm-up and cleaning), presenting the concentrations below 70 000 n cm^{-3} for the readability of the charts. Only a small number of peaks above 70 000 n cm^{-3} are not included in this representation, namely seven points during the warm-up for MI_A357_PERS and two points during the cleaning phase for MI_Cu_PERS. PV_316L_PERS does not present any peaks above 20 000 n cm^{-3}. MI_A357_PERS presents the higher fraction of measurements above the whiskers during warm-up and cleaning because of the reduced density and high volatility of A357 alloy. More detailed results are presented in supplementary materials.

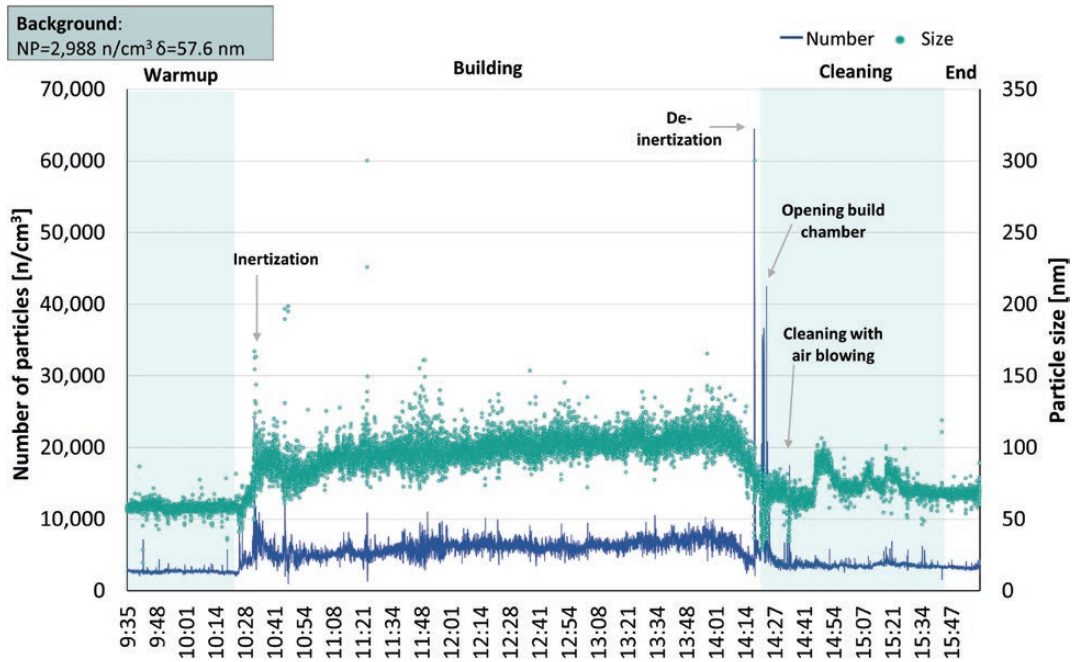

Figure 3. Environmental monitoring of real-time particle release (MI_A357_ENV). Number and size of the particles detected as a function of time and operational phase.

Figure 3 shows the time course of the pattern for particles' concentration and size, highlighting the job tasks corresponding to the release events as registered in the activity diary. MI_A357_ENV followed the standard process workflow and reveals a limited release (<10 000 n cm^{-3} on average with respect to the 2988 n cm^{-3} registered as background), with some significant peaks at the beginning (23 600 n cm^{-3}) and at the end of the manufacturing process (64 400 n cm^{-3}), respectively during the inertisation and de-inertisation of the build chamber, which was supposedly be closed and sealed during these operations. Another release event is associated with the beginning of cleaning operations when the operator opens the build chamber and when the printed job is cleaned by blowing air. It is possible to underline events with a high increase in NP concentration (>30 000 n cm^{-3}), corresponding with the opening of the build chamber. These peaks are associated with a reduction in the particle size (from average diameter of 75 nm to < 28 nm), meaning that during specific activities a significant release of NP with reduced size occurs. Further release events are pointed out by personal monitoring that correspond with the use of a vacuum for cleaning the build chamber and the mechanisms for moving the building plate, and when handling the filter for the argon recirculation.

The process MI_Cu_ENV (Fig. 4) reveals a limited release during warm-up and cleaning, with no significant peaks. The manufacturing phase entails a particle release from around 10 000 to 59 500 n cm^{-3}, also associated with an increase in the particle diameter from 60 to 160 nm. This release interval occurred at the beginning of the building phase, from 11:20 to 12:55, in conjunction with a series of starts and stops of the building process to adjust the set-up parameters (non-ordinary events, see Fig. 1). The first relates to an additional cleaning after the inertisation to remove residues from previous build jobs with different powders (open chamber), while other release events deal with adjustments of process set-up by the operator (closed chamber).

A comparable release pattern also occurred in an additional environmental monitoring performed during the beginning of the building phase of MI_Cu_ENV_2 (Fig. 5a particle number and 5b size of particles) from 11:05 to 12:05. During the build job, two starts and stops were performed to abort some samples owing to an improper power delivery on the baseplate, potentially causing defects on the recoater system. In both processes, some non-ordinary events occurred (see Fig. 1) during these activities, and the operators interacted with the AM device to adjust the building set-up and the build chamber remained sealed with the inertisation maintained as constant.

The process PV_316L_ENV presents a particle concentration during building below 10 000 n cm^{-3}. It is possible to highlight a release event during the warm-up for 5′, where the particle concentration

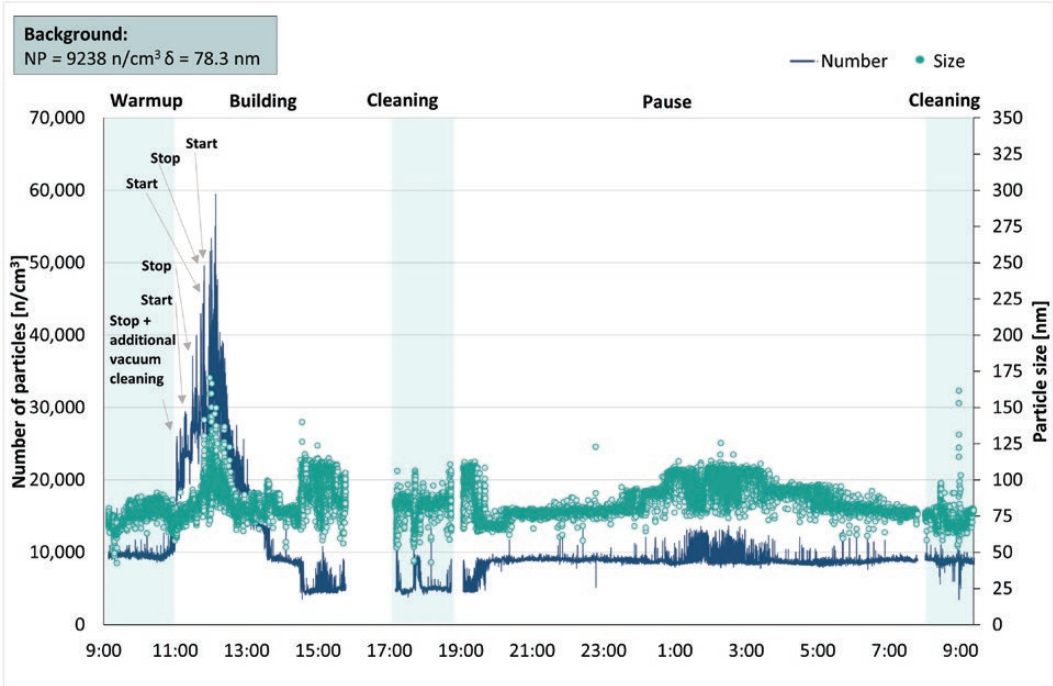

Figure 4. Environmental monitoring of real-time particle release during the whole process (MI_Cu_ENV). Number and size of the particles detected as a function of time and operation phase.

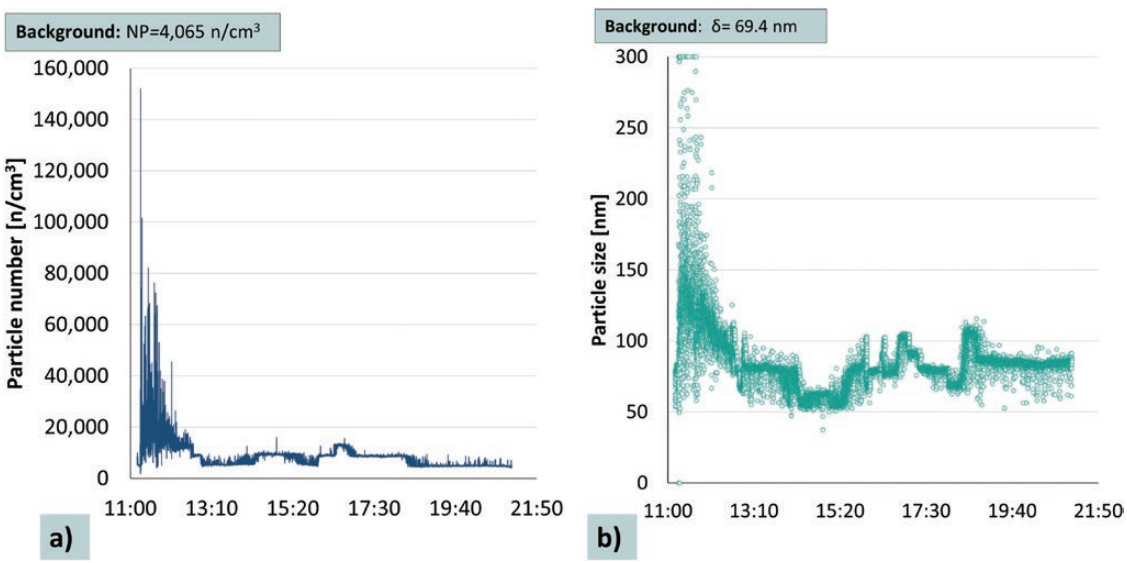

Figure 5. Environmental monitoring of real-time particle release during the building phase (MI_Cu_ENV_2). (a) Number and (b) size of the particles detected as a function of time.

reaches 302 000 n cm^{-3} and the average diameter accounts for 170 nm. This peak corresponded to a non-ordinary event during the warm-up, i.e. the sieving of the residual powders by the operator. The trend for the whole process is reported in supplementary materials.

Personal monitoring confirms the pattern of the environmental one, while the peaks of concentration are

higher since the operator interacts directly with the potential sources of NP.

The process MI_A357_PERS points out several release events associated with specific activities of the operator. During the warm-up (Fig. 6a), the main peaks occur in conjunction with not-ordinary events for checking the overflow, i.e. opening and closing of overflow door (respectively 849 000 n cm^{-3} and 593 000 n cm^{-3}). It is important to highlight that this warm-up was carried out following the conclusion of a previous process, thus the NP released could have been generated during the earlier manufacturing. During cleaning (Fig. 6b), the release events can be associated with job tasks of the standard workflow: opening and closing of the overflow door (respectively 42 700 n cm^{-3} and 47 800 n cm^{-3}), handling of the overflow pipe and container (213 800 n cm^{-3}), use of vacuum for cleaning the joints of the build chamber (81 500 n cm^{-3}) and opening of the filter door (228 000 n cm^{-3}).

The monitoring of MI_Cu_PERS presents a reduced release during the warm-up (Figure available in Supplementary materials), where the concentration is comparable to the background, while during cleaning, the release is in general higher than 10 000 n cm^{-3}. During warm-up and cleaning, no non-ordinary events (as reported in Fig. 1) occurred.

PV_316L_PERS presents a negligible release with respect to the background during warm-up (Fig. 7a),

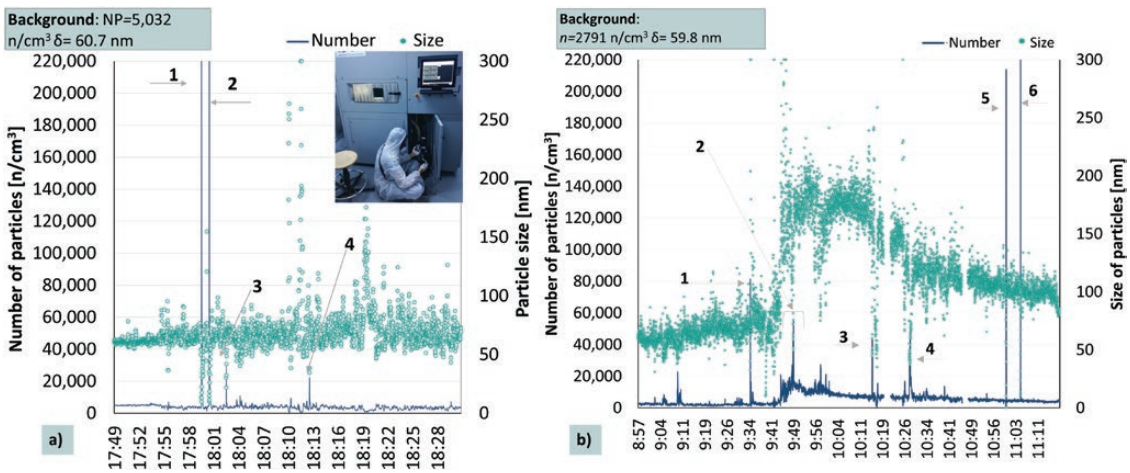

Figure 6. Personal monitoring with use of MI_A357_PERS during (a) warm-up and (b) cleaning. In panel a, release events are: 1) overflow check (849 400 n cm^{-3}), 2) closing overflow door (593 000 n cm^{-3}), 3) opening powder container, and 4) charging powders. In panel (b), release events are: 1) use of vacuum and cleaning of joints; 2) cleaning of components of build chamber and moving plate; 3–4) opening overflow door; 5) mounting pipe connected to overflow container; and 6) opening filter door.

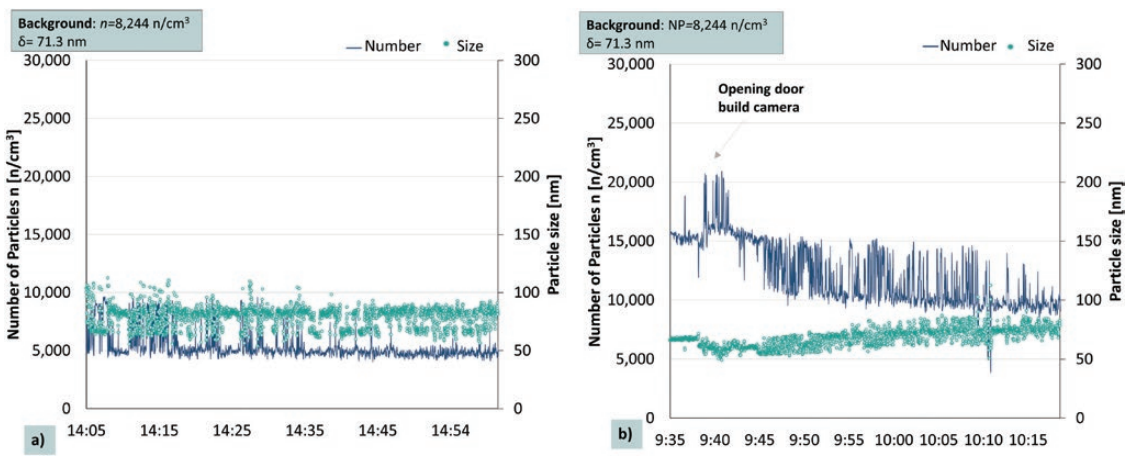

Figure 7. Personal monitoring with use of PV_316L_PERS during (a) warm-up and (b) cleaning. Background measurements are displayed in the top left of the charts.

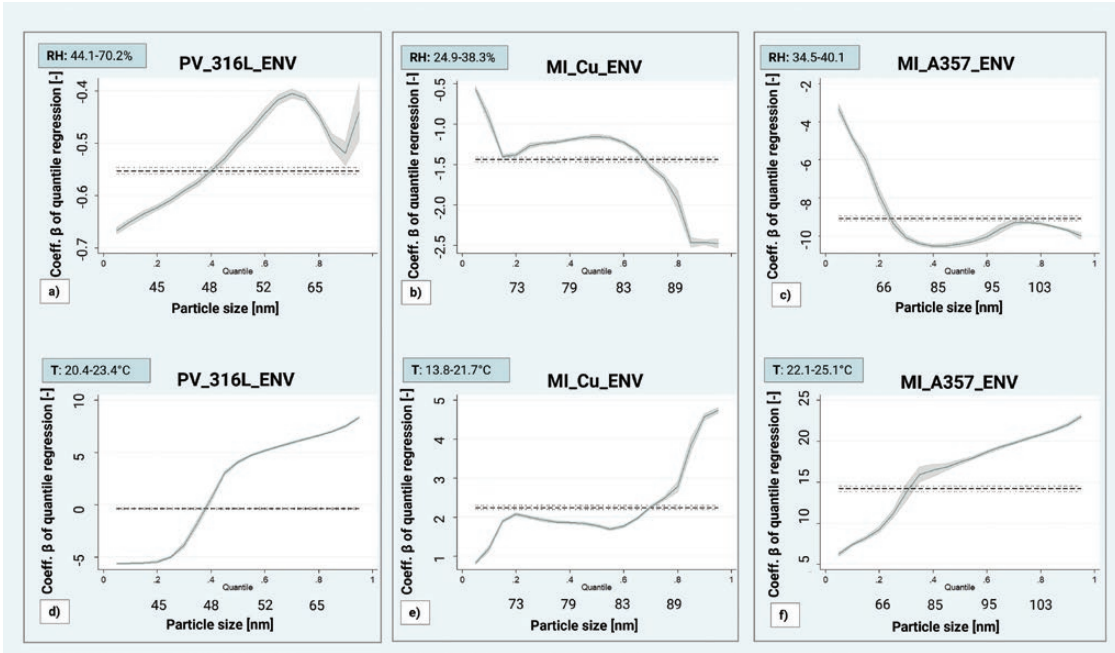

Figure 8. Quantile regression between particle size and relative humidity RH (a–c) and indoor air temperature *t* (d–f).

since in this case, the process followed the standard workflow (Fig. 1), while the monitoring shows a higher concentration during cleaning, especially when the operators open the door of the build chamber (Fig. 7b). The device in UNIPV allows the cleaning initialisation to be performed with the chamber door closed, limiting the release peaks; in fact, the concentration increase when opening the door accounts for an additional measurement of around 5000 n cm^{-3}.

Figure 8 shows the results of the quantile regression between the average size and the relative humidity RH (a–c) and the indoor air temperature *T* (d–f), calculated as reported in Section 2.3. RH and *T* are taken as independent variables and are measured in the AM box during the environmental monitoring of the three processes. Median *T* are similar in all operational phases at UNIPV and during aluminium alloy A357 building at POLIMI, ranging between 21 and 25°C, while lower *T* is measured during pure copper building at POLIMI. Median RH is higher at UNIPV (about 47–60%) compared to POLIMI for both alloys (always lower than 40%).

We can observe negative regression coefficients between the particle size and RH (Fig. 8a–c) and positive regression with the temperature (Fig. 8d–f). This observation is coherent with the inverse correlation generally occurring between HR and *T*. In PV_316L_ENV (Fig. 8a) RH is higher than in MI_Cu_ENV (Fig. 8b) and MI_A357_ENV (Fig. 8c) (average 46% vs 35% and 31% respectively), and the NP released present a shorter median diameter among the monitored processes (49 nm vs 81 nm and 92 nm). In this case, it is possible to observe an increase in the coefficient of quantile regression from −0.7 to −0.4 for different quantiles (until 0.7), which corresponds to a size interval of 10–60 nm, whereas they reduce at higher quantiles and thus for particles larger than 60 nm. The decrease in the regression coefficients in the interval 50–70 nm also occurs in the other two processes. In MI_Cu_ENV the regression coefficient curve increases from −0.5 to −1.5 for particles with a diameter lower than 60 nm (about quantile 0.2), becomes stable in the interval between 70 and 85 (quantiles 0.2–0.6) and presents a decrease up to −2.5 for larger particles. The trend is also comparable for MI_A357_ENV, although in this case the indices highlight more significant negative regression coefficients, ranging from −3 to −10.5. Between particle size and indoor temperature, a positive correlation that increases in parallel with the particle size is observed. The strongest correlation is shown during the process MI_A357_ENV (Fig. 8f), while MI_Cu_ENV presents the weakest one (Fig. 8e).

Discussion

Occupational exposure to metal NP is associated with emerging technologies, and there is still a general lack of structured monitoring data, benchmarks, and reference values. Only provisional limits (nano reference values, NRVs) have been proposed. For powders with

a density higher than 6000 kg m^{-3}, the limit value as a weighted average for the working shift is 20 000 particles cm^{-1}. For a density lower than 6000 kg m^{-3}, the limit accounts for 40 000 particles cm^{-3}. (IFA (German Social Accident Insurance), 2008; Hendrikx and van Broekhuizen, 2013). Notwithstanding, these limits do not consider exposure peaks that could exceed NRV 10–20 times in several operations and for significant durations, such as during the building phase (Fig. 5). For chemical agents lacking short-term and ceiling TLVs, benchmark limit values respectively of 3 and 5 times the average TLV for the working shift are recommended. Taking the above-mentioned values as a reference, although in a low exposure landscape, the monitoring highlighted sudden release events (lasting for around 15–20 s) that are associated with specific actions of the operators or activities of the AM devices exceeding five times the NRVs (ceiling reference). On the other hand, there are no time intervals highlighting a short-term exposure higher than three times the NRV for the monitored processes.

Moreover, the monitoring results show the importance of the measurement time-step: the authors adopted one second, the operative standard mode of the monitoring tool. Longer time steps may be inappropriate to describe the dynamics of the nanoparticle release since the observed peaks can be flattened by average values and consequently underestimated (Spinazzè *et al.*, 2016).

In this regard, evaluating the pattern through prolonged monitoring and associating the peaks of release with specific activities is important so that working procedures can be adjusted and the operators made aware of the potential exposure. The monitoring shows release events corresponding with several actions usually performed during warm-up and cleaning when the operators wear Personal Protection Equipment (PPE), thus the adoption of full-face respiratory mask with filter in class 3 during these phases is effective to mitigate the exposure of the operators.

The presented on-field monitoring identified different release patterns for the used feedstocks. For aluminum A357 alloy and AISI 316L, warm-up and cleaning have the highest particle concentration, when the operators use PPE. The highest peaks for A357 correspond with specific activities, namely opening the overflow door and tanks, cleaning filters, sieving powders, and using the vacuum. AISI 316L present the lowest number of peaks (during powder sieving, when the operators wear PPE) and reduced release during the process. This material has widely been applied in AM, and it is associated with a standard and consolidated process set-up that also ensure controlled release patterns.

A357 is at an advanced research phase and is implemented in industrial settings with proven process parameters. On the other hand, its reduced density represents a significant factor affecting the release of NP, and the highest peaks of concentration among powders are observed. Moreover, the measurement detected further significant peaks that correspond with the inertisation and de-inertisation of the build chamber when the operative procedures allowed entering the room without PPE (Fig. 3).

Pure copper is not industrially applied as much as stainless steel and aluminium powders because the high reflectivity coupled with high thermal diffusivity makes its L-PBF processability very unstable, resulting in high porosity, oxidation and poor mechanical properties of the manufactured component (Colopi *et al.*, 2019). The set-up of the parameters for pure copper powder is still an open and ongoing investigation along with the appropriate selection of the laser beam source: green laser or more recently blue lasers (Hori *et al.*, 2021), pulsed wave or continuous wave lasers, single mode or multi-mode/dynamic beam shaping sources are the latest devices to overcome challenges in L-PBF of pure copper. Throughout the experimental activity, the investigation of pure copper processability was carried out using ultra-high volumetric energy densities (Jiang *et al.*, 2021), which led to a significant level of vaporisation detected during the personal and environmental monitoring phases. The monitored data in Fig. 4 highlight that the building phase presents a significant release, also confirmed by the additional measurements in Fig. 5. The release occurred during the deposition of the first layers at the beginning of the build job. Here, the testing of ultra-high energy density conditions likely led to excessive stainless steel baseplate vaporisation along with improper melting and vaporisation of pure copper powder. The initial process instability was attributed to the scarce number of layers deposited which entailed a direct remelting and vaporisation of the baseplate. As shown in Supplementary Table SM1, the energy density necessary for a proper L-PBF of stainless-steel powder is two orders of magnitude lower than that tested with pure copper powder. This attests to the exposure of the baseplate to vaporisation caused by the choice of process parameters. Along with the substrate, pure copper powder itself is the most sensitive alloy to vaporisation with the given process parameters. In fact, as reported in Supplementary Table SM1, pure copper powder shows the highest estimated vaporisation fraction (m′, accounting for 0.68 respect to 0.12 of AISI 316L and 0.22 of A357) among the treated alloys. Further measurements are needed to better characterise these release events and to improve the safety procedures and the features of the AM devices. In fact, during building, no PPEs are usually adopted, and the operators may be exposed to a significant number of NP for long intervals due to the needed

interaction with the AM device to adjust set-up parameters and restore the building process. Moreover, these results also provide inputs for the design of the AM devices, introducing new requirements to limit the release of nanoparticles. The sealing of the chamber door needs to be improved to contain the nanoparticles generated by the printing phase, and the filtering of the fumes and argon from the build chamber during the de-inertisation needs to be adapted to limit the flows of nanoparticles.

The monitoring campaign confirms that the main NP exposures correspond to several activities that, in the current design of AM devices, are carried out manually: namely handling the powders for charging, cleaning the machine and the environment, and sieving the powders for their re-use. In addition, the monitoring highlights potential risks during the building phase, when adjustments of process parameters are made by the operators. This risk is more significant for research activities working with open-architecture systems on experimental set-ups that require process parameter optimisation but may occur also in industrial settings in case of malfunctions or non-ordinary events.

The presented measurements deal with three different powders with peculiar toxic profiles. AISI 316L (used at UNIPV) contains cobalt, chromium and nickel, the latter being carcinogenic by inhalation. The presence of these metals was observed by the authors in POLIMI and UNIPV AM facilities in previous monitoring campaigns (Oddone *et al.*, 2022). The gravimetric techniques applied in that work confirmed the results of previous monitoring in AM working environments (Ljunggren *et al.*, 2019), highlighting negligible metal concentrations for both inhalable and respirable particles in comparison to available TLVs. Concerning pure copper powder and aluminum A357 alloy (used at POLIMI) no carcinogenic effects are known, but they are sensitising agents and can induce asthma, as reported in safety data sheets according to REACH-CLP legislation (European Parliament, 2008).

On the other hand, the evaluation of the toxicity metals at the nanometer scale, which is halfway between classical and quantum physics (Medici *et al.*, 2021), is still at a preliminary research phase, and there is not a complete agreement on the potential health hazard associated with the NP generated as by-products during AM processes (Wang *et al.*, 2021; Vallabani *et al.*, 2022).

The approach based on gravimetric analysis does not provide a complete characterisation of the released powder (Oddone *et al.*, 2022). The number per unit of air volume, the size and shape of the particles, and the active surface (i.e. the surface area that becomes available for direct interactions with the biological systems) are more significant and the potential toxicity usually increases as the size of the particles decreases (Nanoparticle toxicology, in Casarett and Doull's Toxicology, 2019). As an example, a recent study showed a more intense lung inflammatory reaction in experimental animals when exposed to TiO_2 NP with a 20 nm diameter compared to exposure to particles of the same material with a 250 nm diameter, while a similar dose- response was observed when, for each of the two particle sizes, the dose was expressed as a surface area (Oberdörster *et al.*, 2005). Being smaller than single cells and their organelles, exposure to NP can lead to oxidative stress, cellular dysfunction and toxicity, since the human immune system is not designed to recognise and defend against particles smaller than 1 μm (Medici *et al.*, 2021). Moreover, NP could promote macrophages, neutrophils and dendritic cell activation, leading to secretion of pro-inflammatory cytokines and thus to potential pathologic consequences, such as lung inflammation and fibrosis (Leikauf *et al.*, 2020).

Recent studies in Northern Europe, with results similar to ours in terms of concentration and size of metal NP, demonstrated skin and systemic exposure (detected in urine) in AM facility workers, as well as consequent alterations in indicators of inflammation and liver function, with normalisation after exposure prevention interventions (Ljunggren *et al.*, 2019, 2021; Assenhöj *et al.*, 2021), stressing once again the need for adequate methods of assessment and exposure control.

According to these considerations, with some attempts to systematise using a control banding (CB) qualitative approach, the exposure assessment has been made considering the toxicological characteristics of parental materials making up the powder alloys, the toxicological and dimensional characteristics of NP produced in AM processes and production process features (Sousa *et al.*, 2021). However, the CB approach for qualitative assessment (Zalk *et al.*, 2009; Sousa *et al.*, 2019), does not consider the possible dependence of particles concentration and size on microclimatic parameters. Relative humidity influences the nanoparticle deposition rate, with a significant inverse correlation for particles with a diameter up to 70 nm (Wang *et al.*, 2017). The monitoring in UNIPV and POLIMI confirmed the negative correlation between particle size and relative humidity, whose magnitude is higher for particles smaller than 70 nm (Fig. 8a–c). This observation suggests a potential action of relative humidity in keeping the particles separate, preventing the aggregation mechanism and consequent deposition. Further measurements under different conditions are needed to better assess the role of microclimatic parameters on the particle size and concentration. Nevertheless, the results presented in this work suggest an impact on the potential exposure

to NP in AM facilities and thus they deserve to be considered in the risk assessment and controlled during work processes.

Limitations of the study

The results presented in this work deal with a series of alloys and AM devices, with different level of maturity and physical properties, aiming to provide an overview of the nanoparticle release of L-PBF. Nevertheless, the monitoring campaign included six processes representing a limited sample characterised by different variables, among which were: boundary conditions, operator in charge of managing the activities, length, and complexity of the job. Therefore, the results may be affected by the above-mentioned variables, and further measurements including a larger number of processes are needed to provide a consistent overview and reference benchmarks. Moreover, the performed on-field monitoring would require further measurements to provide a comprehensive chemical characterisation of the nanoparticulate. Nevertheless, some considerations can be based on the identification of the nanoparticle release pattern according to the activities of the operators and process data.

Another limitation of the study lies in the adoption of Testo DiSCMini, which allows the implementation of personal monitoring but presents a lower level of precision than other instruments (e.g. condensation particle counters and scanning mobility particle sizers) and can introduce an error rate up to ± 30% (Todea *et al.*, 2017). Nevertheless, the main outcomes of the study deal with peaks exceeding the NRV up to 20 times, thus they are not affected by the precision of the measure. Further monitoring adopting more accurate measurement devices would allow the results to be validated.

Despite these limitations, this work contributes to the characterisation of the potential nanoparticle release during L-PBF processes and provides preliminary indications for improving the process management and reducing the risks for the operators.

Conclusions

The results show a controlled release in the monitored sites with a limited average exposure of the operators, wearing PPE when the build chamber is open and when handling powders. On the other hand, the prolonged real-time measurements highlight significant peaks of NP concentration corresponding to specific actions. The highest release for AISI 316L and A357 (widely adopted in AM) occurs during warm-up and cleaning, when operators wear PPE. Pure copper processes show a significant concentration during building when operators do not wear PPE. However, pure copper represents an uncommon powder feedstock in the L-PBF framework, whose processability is an ongoing research topic.

These outcomes represent useful inputs to fine-tune the working procedures and features of the devices to further improve the level of safety of AM. The potential strategies may rely on introducing higher level of automation for specific operations during cleaning and warm-up, increasing the ventilation rate for removing NP in relation to the foreseen release events, controlling the temperature and relative humidity to foster the nanoparticle aggregation.

Further monitoring sessions of different sites and conditions are needed to increase the robustness of the results towards the definition of process benchmarks and release potential of the AM devices with the current technologies.

Conflict of interest

There are no potential conflicts of interest, and the authors have nothing to disclose.

Data Availability

The data underlying this article cannot be shared publicly due to confidential issues. The data will be shared on reasonable request to the corresponding author.

Author's contribution

R.P.: conceptualization, methodology, on-site monitoring and elaboration of the data, visualization, writing original draft. *F.G.*: organization of the on-site monitoring, writing original draft. *A.C.*: organization of the on-site monitoring, review of the drafted manuscript. *E.B.*: review of the drafted manuscript. *B.P.*: conceptualization, review of the drafted manuscript. *E.O.*: conceptualization, methodology, supervision, writing original draft

Supplementary Data

Supplementary data are available at *Annals of Work Exposures and Health* online.

References

American Conference of Governmental Industrial Hygienists. (2021) TLVs and BEIs. Available at https://portal.acgih.org/s/store#/store/browse/detail/a154W00000BOag7QAD. Accessed 10 May 2022.

Assenhöj M, Ward LJ, Ghafouri B *et al.* (2021) Metal exposure from additive manufacturing and its effect on the nasal lavage fluid proteome—a pilot study. *PLoS One*; **16**: e0256746.

Hendrikx B, van Broekhuizen P. (2013) Nano reference values in the Netherlands. *Gefahrstoffe Reinhalt Luft*; **10**: 407–14.
Bengalli R, Gualtieri M, Capasso L *et al*. (2017) Impact of zinc oxide nanoparticles on an in vitro model of the human air-blood barrier. *Toxicol Lett*; **279**: 22–32.
Böckin D, Tillman A-M, Tillman A-M. (2019) Environmental assessment of additive manufacturing in the automotive industry. *J Clean Prod*; **226**: 977–87.
Comité Européen de Normalisation (CEN). (2021) EN 143:2021 Respiratory protective devices—particle filters—requirements, testing, marking.
Chen R, Yin H, Cole IS *et al*. (2020) Exposure, assessment and health hazards of particulate matter in metal additive manufacturing: a review. *Chemosphere*; **259**: 127452.
Colopi M, Demir AG, Caprio L *et al*. (2019) Limits and solutions in processing pure Cu via selective laser melting using a high-power single-mode fiber laser. *Int J Adv Manuf Technol*; **104**: 2473–86.
Duffin R, Tran L, Brown D *et al*. (2007) Proinflammogenic effects of low-toxicity and metal nanoparticles in vivo and in vitro: highlighting the role of particle surface area and surface reactivity. *Inhal Toxicol*; **19**: 849–56.
European Parliament. (2008) Regulation (EC) No 1272/2008 Classification, labelling and packaging of substances and mixtures, amending and repealing Directives 67/548/EEC and 1999/45/EC, and amending Regulation (EC) No 1907/2006 (Text with EEA relevance). Available at https://eur-lex.europa.eu/legal-content/en/TXT/?uri=CELEX%3A32008R1272. Accessed 10 May 2022.
Fierz M, Houle C, Steigmeier P *et al*. (2011) Design, calibration, and field performance of a miniature diffusion size classifier. *Aerosol Sci Technol*; **45**: 1–10.
Fonseca AS, Maragkidou A, Viana M *et al*. (2016) Process-generated nanoparticles from ceramic tile sintering: emissions, exposure and environmental release. *Sci Total Environ*; **565**: 922–32.
Hori E, Sato Y, Shibata T *et al*. (2021) Development of SLM process using 200 W blue diode laser for pure copper additive manufacturing of high density structure. *J Laser Appl*; **33**: 012008.
IFA (German Social Accident Insurance). (2008) Criteria for assessment of the effectiveness of protective measures. Ed. Institut für Arbeitsschutz der Deutschen Gesetzlichen Unfallversicherung (IFA), Sankt Augustin.
International Organization for Standardization. (2019) ISO/ASTM52921—13 Standard terminology for additive manufacturing—coordinate systems and test methodologies.
International Organization for Standardization (2021) ISO/ASTM 52900 Additive manufacturing — General principles — Fundamentals and vocabulary.
Jensen ACO, Harboe H, Brostrøm A *et al*. (2020) Nanoparticle exposure and workplace measurements during processes related to 3D printing of a metal object. *Front Public Health*; **8**: 608718.
Jiang Q, Zhang P, Yu Z *et al*. (2021) A review on additive manufacturing of pure copper. *Coatings*; **11**: 740.
Kolb T, Beisser R, Schmidt P *et al*. (2017) Safety in additive manufacturing: fine dust measurements for a process chain in Laser beam melting of metals. *RTejournal Forum für Rapid Technologie*; urn:nbn:de:0009-2-46268.
Kreyling WG, Hirn S, Möller W *et al*. (2014) Air–blood barrier translocation of tracheally instilled gold nanoparticles inversely depends on particle size. *ACS Nano*; **8**: 222–33.
Kuijpers E, Bekker C, Brouwer D *et al*. (2017) Understanding workers' exposure: systematic review and data-analysis of emission potential for NOAA. *J Occup Environ Hyg*; **14**: 349–59.
Leikauf GD, Kim S-H, Jang A-S. (2020) Mechanisms of ultrafine particle-induced respiratory health effects. *Exp Mol Med*; **52**: 329–37.
Ljunggren SA, Karlsson H, Ståhlbom B *et al*. (2019) Biomonitoring of metal exposure during additive manufacturing (3d printing). *Saf Health Work*; **10**: 518–26.
Ljunggren SA, Ward LJ, Graff P *et al*. (2021) Metal additive manufacturing and possible clinical markers for the monitoring of exposure-related health effects. *PLoS One*; **16**: e0248601.
Medici S, Peana M, Pelucelli A *et al*. (2021) An updated overview on metal nanoparticles toxicity. *Semin Cancer Biol*; **76**: 17–26.
Mellin P, Jönsson C, Åkermo M *et al*. (2016) Nano-sized by-products from metal 3D printing, composite manufacturing and fabric production. *J Clean Prod*; **139**: 1224–33.
Nanoparticle toxicology, in Casarett and Doull's Toxicology. (2019), 9th edn. New York: McGraw Hill.
National Institute of Occupational Safety and Health. (2007) Pocket guide to chemical hazards. Available at https://www.cdc.gov/niosh/docs/2005-149/pdfs/2005-149.pdf. Accessed 10 May 2022.
Niaki MK, Torabi SA, Nonino F. (2019) Why manufacturers adopt additive manufacturing technologies: the role of sustainability. *J Clean Prod*; **222**: 381–92.
Oberdörster G, Oberdöörster E, Oberdörster J. (2005) Nanotoxicology: an emerging discipline evolving from studies of ultrafine particles. *Environ Health Perspect*; **113**: 823–39.
Occupational Safety and Health Administration. (2020) Permissible Exposure Limits. Available at https://www.osha.gov/annotated-pels. Accessed 10 May 2022.
Oddone E, Pernetti R, Fiorentino ML *et al*. (2022) Particle measurements of metal additive manufacturing to assess working occupational exposures: a comparative analysis of selective laser melting, laser metal deposition and hybrid laser metal deposition. *Ind Health*; **60**: 371–86.
Van Broekhuize P, Van Veelen W, Streekstra W-H *et al*. (2012) Exposure limits for nanoparticles: report of an international workshop on nano reference values. *Ann Occup Hyg*; **56**: 515–24.
Shi X, Chen R, Huo L *et al*. (2015) Evaluation of nanoparticles emitted from printers in a lean chamber, a copy center and office rooms: ealth risks of indoor air quality. *J Nanosci Nanotechnol*; **15**: 9554–64.
Sousa M, Arezes P, Silva F. (2019) Nanomaterials exposure as an occupational risk in metal additive manufacturing. *J Phys Conf Ser*; **1323**: 012013.
Sousa M, Arezes P, Silva F. (2021) Occupational exposure to ultrafine particles in metal additive manufacturing: a qualitative and quantitative risk assessment. *IJERPH*; **18**: 9788.

Spinazzè A, Cattaneo A, Limonta M *et al*. (2016) Titanium dioxide nanoparticles: occupational exposure assessment in the photocatalytic paving production. *J Nanopart Res*; **18**: 151.

Todea AM, Beckmann S, Kaminski H *et al*. (2017) Intercomparison of personal monitors for nanoparticles exposure at workplaces and in the environment. *Sci Total Environ*; **60**: 929–45.

Vallabani NVS, Alijagic A, Persson A *et al*. (2022) Toxicity evaluation of particles formed during 3D-printing: cytotoxic, genotoxic, and inflammatory response in lung and macrophage models. *Toxicology*; **467**: 153100.

Wang X, Vallabani NVS, Giboin A *et al*. (2021) Bioaccessibility and reactivity of alloy powders used in powder bed fusion additive manufacturing. *Materialia*; **19**: 101196.

Wang Y, Chen L, Chen R *et al*. (2017) Effect of relative humidity on the deposition and coagulation of aerosolized SiO2 nanoparticles. *Atmos Res*; **194**: 100–8.

Zalk DM, Paik SY, Swuste P. (2009) Evaluating the Control Banding Nanotool: a qualitative risk assessment method for controlling nanoparticle exposures. *J Nanopart Res*; **11**: 1685–704.